Design and analysis of bio-inspired cellular structures with variable relative density produced with fused filament fabrication

André Francisco Azevedo Oliveira

azevedooliveira@tecnico.ulisboa.pt

Instituto Superior Técnico, Universidade de Lisboa, Portugal

November 2021

Abstract

Cellular structures are interconnected networks of solid struts or plates, which give shape to the edges and faces of unit cells. They are characterized by excellent properties, such as strength, high stiffness and energy absorption, maintaining a low weight. Hence, they are extensively used in many industries and applications. An example is composite sandwich panels, where the core between the two skins has a cellular structure.

Within these cellular structures, lattices are a type of 3D cellular structure, which is obtained by the repetition of a unit cell. There are several types of unit cells that give rise to architecture 3D lattice structures, being an example the triply periodic minimal surfaces (TPMS) type, as the one designed and studied in this work. The unit cell was bio-inspired, as it happens with many unit cells, i.e., they mimic some structures present in nature. In this work, the unit cell was inspired by a sea urchin.

The aim of this research was to evaluate the mechanical properties of lattice structures, all composed of the unit cell designed, in sandwich panels and cubic structures. Also, three different values of relative density of the unit cell were used, to study the influence of the relative density of the lattice structures on their mechanical properties. The values of relative density used were 0.20, 0.25 and 0.30.

Both experimental and numerical analyses were performed in both compression and three-point bending tests. The numerical analyses were made using the Siemens NX software. The experimental specimens were previously manufactured by a fused filament fabrication (FFF) process on a commercial 3D printing machine, using polylactic acid neutral PLA-N.

The results obtained suggest that in the compression tests the reaction load, stiffness and energy absorbed increase with increasing the relative density, in both experimental and numerical results. The 0.30 specimens showed the best results, mainly in the numerical simulations. The failure observations on the specimens have shown that the specimens failed at half-height of the unit cells. Concerning the bending tests, contrary to the compression ones, the mechanical properties decreased with increasing the relative density. However, there was a small variation of the results, which led to the conclusion that to have a greater variation of properties, there must be greater variation of the relative density of the cells of the core. The failure behaviours observed in bending specimens were associated with details presented at specific printed layers of the unit cells, probably related to overhangs limitations.

In conclusion, the geometrical parameters of the unit cells design have a greater influence on the mechanical properties when subjected to compression, than when subjected to bending in the core of sandwich panels, mainly regarding the region of connection between cells.

Keywords: Lattice structures, sandwich panels, additive manufacturing, relative density, compression test, three-point bending test, numerical simulations

1. Introduction

In structural engineering, the main objective is to design parts with good mechanical properties, such as high stiffness and strength but with the lowest weight possible. Cellular structures are a good example of these characteristics. In specific, an example of a cellular structure is the core of a sandwich structure/panel. Due to their versatility, these structures are used in many industries, keeping a low relative density. To potentiate their properties, the main alterations in the design process that can be made are related with geometrical variations of the unit cell that compose the core of the panel.

Cellular structures can be manufactured in many ways. Additive manufacturing (AM) has proven to be advantageous due to the design complexity and flexibility that can be achieved and it has had an increasing influence on the research and development of cellular structures. Fused Filament Fabrication (FFF), which is part of the Material Extrusion category of AM, was the manufacturing process used in this thesis.

Recently, cellular structures had an outstanding development, namely the 3D lattice structures, which are a type of cellular structures. Lattices are composed of unit cells, which can have various shapes and designs. Within these, the triply periodic minimal surfaces (TPMS), which are a type of unit cells, have been an object of research, obtaining great results and showing good potential.

In this thesis, the main objective is to analyse the effect of relative density on the mechanical properties of cubic samples and sandwich panels made by PLA-N and composed of TPMS unit cells by carrying out compression and three-point bending (3PB) experimental tests, respectively.

2. Literature review

Cellular solids are an interconnected network of solid struts or plates forming the edges and faces of cells. The typical structures of cellular solids are the two-dimensional honeycombs, for which the most commonly used is the arrangement of hexagonal cells. Also, the cells can be packed in three dimensions to fill space, such as foams and/or lattice materials [1].

Lattices, unlike foams, have a periodic geometry or arrangement, that can be defined by a small number of design parameters. They are characterized by a unit cell with certain symmetry elements, which is repeated. Lattices can have two-dimensional cells, like honeycombs, but normally, the cells are comprised of struts and nodes in a three-dimensional way.

By tailoring the geometry of the unit cell, whereas the base material is the same, it is possible to obtain very different properties depending on the application, such as stiffness, strength, low density, permeability and thermal conductivity [2]. Lattices have applications in many areas, such as automotive, aerospace and biomedical areas.

One typical example of application of lattice structures are the sandwich panels, which are a type of composite panel. It consists of two thin solid face-sheets at the top and bottom of the panel separated by a lightweight core that is thicker than the two others [3]. It is at the core where the lattice structures are used. An example of a sandwich panel is presented in Figure 1.

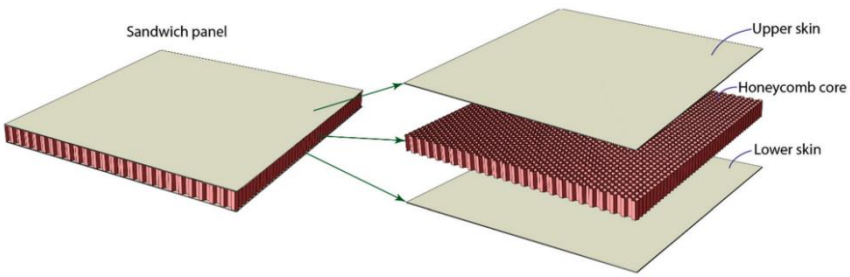

Figure 1: Example of a sandwich panel [4]

These structures are widely used in aerospace, marine, sporting and automotive applications due to the lightweight design of the core, high stiffness, excellent thermal insulation and high energy absorption capability [3].

Regarding the architecture of 3D lattice structures, Benedetti et al. [2] classifies them into three different unit cell types. The most common are the “Strut-based lattices”, where the nodes are located at the vertices or edges of the unit cells, or sometimes in the interior, which are connected by slender straight members normally called struts (or beams). Also, there are two more types of unit cells, the “Skeletal-TPMS based lattices” and “Sheet-TPMS based lattices”, both based on triply periodic minimal surfaces (TPMS), that are created, either by thickening the minimal surface to create “Sheet-TPMS based lattices” or by solidifying the volumes enclosed by the minimal surfaces to create “Skeletal-TPMS based lattices”. Examples of the three types of unit cells are presented in Figure *2*.

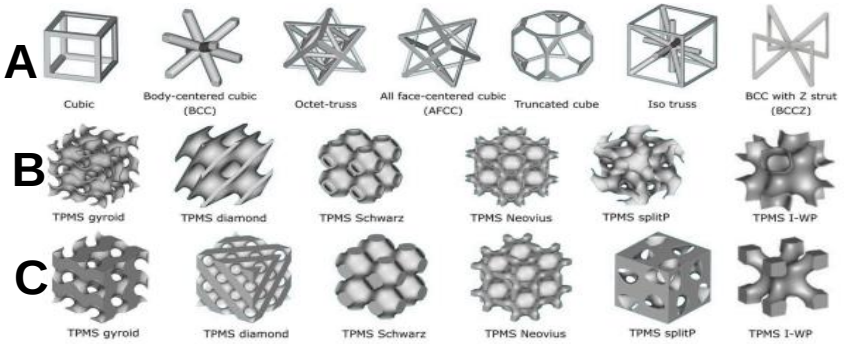

Figure 2: Types of unit cells (A) Strut-based lattices (B) Sheet-TPMS based lattices (C) Skeletal-based lattices [2]

The TPMS unit cell designed and analysed in this thesis was based on bioinspired cells made by Kumar et al. [5], as presented in Figure 3. These were bio-mimicked structures of a sea urchin shape because they are mechanically stable load-bearing structures. Kumar et al. [5] always used the same relative density (0.32) in cubic specimens subjected to compression tests. These had different topologies, which are open-cells, local closed cells and global closed cells, with two global dimensions, 8 x 8 x 8 mm cells size compared to 10.7 x 10.7 x 10.7 mm cells size.

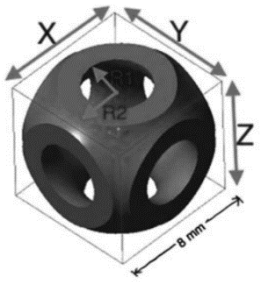

Figure 3: TPMS unit cell made by Kumar et al. [6]

Commonly known as 3D printing, Additive Manufacturing (AM) encompasses all technologies capable of creating three-dimensional objects, through layers deposited successively on top of each other. AM processes can be advantageous over traditional manufacturing processes, as they cause little waste, namely in terms of material, thus being able to reduce the final costs of the products and also reduce the lead time of a project [7]. Accordingly to the standard ISO/ASTM 52900, there are seven AM processes categories, as they are: binder jetting, directed energy deposition, material extrusion, material jetting, powder bed fusion, sheet lamination and vat photopolymerization [8].

Structures with sophisticated cellular architecture can be fabricated with few approaches, being the material extrusion processes the most efficient and viable solution. Specifically, the Fused Filament Fabrication (FFF) is a process capable of producing good structures, in a relatively short time and without many necessary resources.

3. Materials and methods

The design of the unit cell, like geometry and relative density were studied and chosen, as well the FFF printing parameters to produce the cubic and sandwich panels specimens. Three values of relative density, 0.20, 0.25 and 0.30 were chosen to study the variation of some mechanical properties.

The constituent material of the specimens manufactured by FFF process was polylactic acid neutral PLA-N. It is the most researched and used biodegradable aliphatic polyester (thermoplastic polymer) and is well known for its high-strength and high-modulus.

Unit cell and specimens design

A total of six specimens (three cubic specimens and three sandwich panels specimens), all with the same unit cell design. These designs were made using the CAD software Solidworks 2019.

The unit cell dimensions used in this study were chosen considering a few manufacturing constraints, such as the printing times, specifically not exceeding about ten hours, the global dimensions between $12^3\ mm$ and $15^3\ mm$ and as a first approach, the global dimensions used by Kumar et al. [5], as well the quality of the walls and surfaces printed. The global dimensions chosen were $13.5 * 13.5 * 13.5\ mm$.

The relative density of the unit cell was obtained as follows:

$$\rho_{rel} = \frac{V_{unit\ cell}}{V_{enclosure}} \tag{3.1}$$

Where, $V_{unit\ cell}$ is the volume occupied by the unit cell itself, and $V_{enclosure}$ is the volume of a cube enclosure with the same global dimensions of the unit cell.

Among all the geometrical parameters of the unit cell, there are three that show clear diferences between the three unit cells. These are the spherical shell thickness, the circular crowns of connection área between unit cells, represented in blue in Figure 4 and the area represented in yellow. Table *1* shows the different values of the three parameters between the three unit cells.

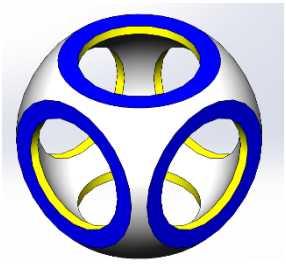

Figure 4: Example of an unit cell, with emphasis on certain geometrical parameters

Table 1: Geometrical parameters of the three unit cells designed for each relative density

Relative density	Spherical shell thickness [mm]	Contact faces between cells [mm]	Thickness of circular holes [mm]
0.20	1.5	1.45	0.75
0.25	1.95	1.45	1.32
0.30	2.25	1.83	1.41

Figure 5 presents an example of a cubic compression specimen and a sandwich panel specimen for bending tests. The global dimensions of the cubic specimens are 40.5 x 40.5 x 40.5 mm, consisting of three unit cells on each edge of the specimen, obtaining a total of 27 unit cells per compression specimen. Concerning the sandwich panels, the global dimensions are presented in Figure 5 consisting of 13 unit cells in the length direction and 3 unit cells in the width direction, resulting in a total number of unit cells equal to 39. The face-sheets have a thickness equal to 1.5 mm.

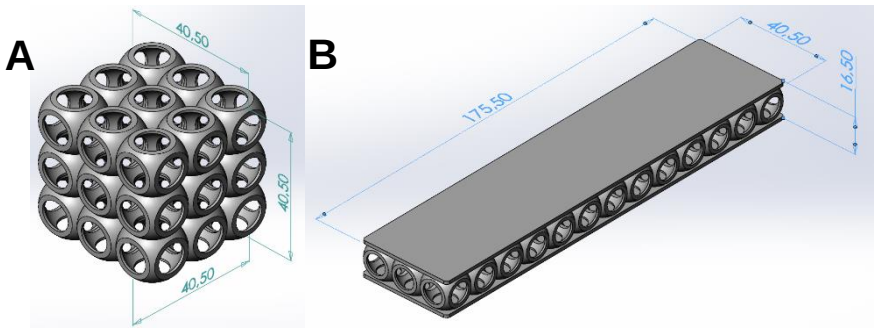

Figure 5: Examples of specimens designed (A) cubic compression specimen (B) bending sandwich panel specimen

Specimens manufacture

The specimens were manufactured using FFF technology, in a Ultimaker 3 machine. Firstly, the specimens models were created in Solidworks and then exported as a STEP file. Then the slicer software, the CURA software from Ultimaker, slices the model into layers with all the parameters and generates a G-code ready to be read by the 3D printing machine.

The material used was the PLA-N, supplied by Filkemp. The diameter nozzle used was 0.4 mm.

Regarding the manufacturing parameters, firstly, several tests were performed, iteratively, to achieve the best quality for all specimens, namely the surface quality, the bonding between cells, the dimensions and also to minimize and avoid other defects as a result of the printing of the specimens.

Figure 6 shows examples of compression and bending specimens being printed.

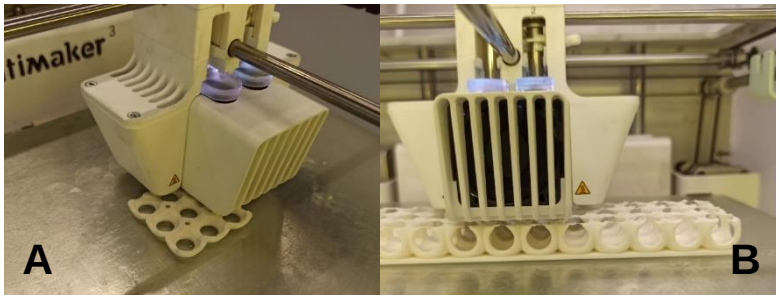

Figure 6: Specimens being manufactured (A) cubic compression specimen (B) sandwich panel bending specimen

Experimental tests methodology

For both compression and 3-point bending tests, three specimens of each of the three relative densities were manufactured.

The compression experimental tests were performed in agreement with the standard ASTM D1621 – 16 (Standard Test Method for Compressive Properties of Rigid Cellular Plastics) [9]. The 3 Point Bending tests (3PB tests) were performed according to the standard ASTM C393 – 00 (Standard Test Method for Flexural Properties of Sandwich Constructions) [10].

In the bending experimental tests, the midspan loading was 110 mm. The overhang distance, i.e., the horizontal distance between the beginning of the specimen and the bottom rollers, was 32,75 mm for each side.

For both experimental tests, the equipment used was an Instron 3369 with a load cell of 50 kN. For all the bending tests performed, the upper roller moved downward at a speed of $2.5\ mm/min$. The two bottom rollers were fixed. The load-displacement data from all tests were obtained with the Bluehill software.

Numerical analyses

For the numerical analyses made in this work, it was used the software Siemens NX, version 1957, which is a Finite Element Method (FEM). To do all the analyses and the calculations, the software needs three different files: *part*, *fem* and *sim* files, for each relative density in both compression and bending tests, as can be seen in Figure 7 and Figure 8, respectively. After they have been made, a solution solver, which defines the parameters and conditions for each case, is used. Both analyses used an enforced displacement equal to 3 mm, applied in the upper surface of the compression specimen and in the top roller of the bending tests.

Figure 7: Compression part, fem and sim files

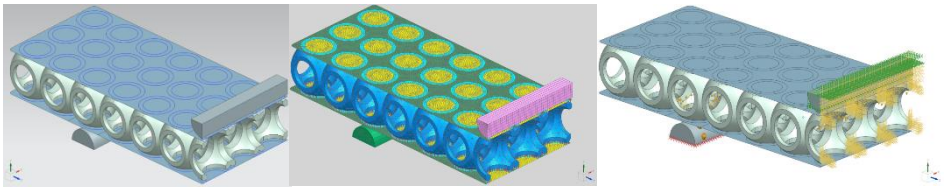

Figure 8: Bending part, fem and sim files

In order to have accurate results from the numerical analyses, mesh refinement is performed in the fem files of each specimen. The mesh refinement studies were made in a specific node for both numerical analyses. The convergence criterion used to guarantee the accuracy of the elements sizes of fem and the von Mises stresses was defined as not exceeding 5% of the difference between von Mises stress on the node analysed. For both compression and bending simulations, the choice of the element size for all specimens was 1.0 mm.

4. Results and discussion

Numerical simulations results

For both compression and bending numerical simulations, a linear elastic anlysis was made in Siemens NX, with an enforced displacement of 3 mm. Figure 9 presents the results of FEA, specifically the maximum von Mises stress, for an example of compression specimen and bending specimen, on the left and right sides, respectively.

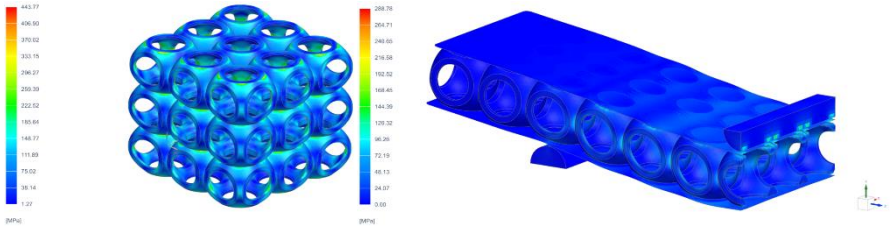

Figure 9: Results of von Mises stress in examples of compression and bending specimens

Using the numerical load *vs* displacement curves, it is possible to observe the reaction loads on the specimens, as well as to obtain the stiffness *K* and the energy absorbed. These vertical forces correspond to a vertical enforced displacement of 3 mm. The stiffness *K* is the slope of the load *vs*

displacement curve and the energy absorbed is the area below the curve. These mechanical properties can be observed in Table 2.

Table 2: Numerical results and mechanical properties calculated for compression and bending simulations

	Relative density	Maximum $\sigma_{V.M.}$ [MPa]	Reaction load [N]	Stiffness *K* [N/mm]	Energy absorbed [J]
Compression specimens	0.20	443.77	17126.51	5708.84	25.690
	0.25	500.67	22817.62	7605.87	34.226
	0.30	569.56	32009.91	10669.97	48.015
Bending specimens	0.20	288.78	1311.80	437.27	1.968
	0.25	311.06	1498.86	499.62	2.248
	0.30	300.37	1746.52	582.17	2.620

Experimental results

The experimental results of the eighteen specimens, nine compression specimens and nine bending specimens, were divided into six groups, which correspond to each relative density in both experimental tests. The experimental results obtained correspond to the maximum load applied to that specimen. However, just the average experimental results are presented in Table 3.

Table 3: Experimental results and mechanical properties calculated for compression and bending tests

	Relative density	Displacement [mm]	Maximum load [N]	Stiffness *K* [N/mm]	Energy absorbed [J]
Compression specimens	0.20	2.386	3981.184	1715.233	6.118
	0.25	2.322	4478.632	1924.360	7.409
	0.30	2.812	7323.350	2606.790	14.675
Bending specimens	0.20	2.350	725.002	312.319	0.938
	0.25	2.883	1019.271	356.178	1.696
	0.30	4.055	1341.679	333.282	3.441

Failure observations

After the experimental tests, two failure modes were observed in the compression specimens. They were characterized by the failure of the upper layer/row of unit cells or the failure of the lower row. Then the failures normally propogated to the middle and the symmetric layer to the first to fail. Figure 10 shows a compression specimen being tested and the beginning of fractures at half-height of the unit cells, in the smallest section, inside the red areas. After some relatively low enforced displacement, these points of the unit cells started to bend and then started to crack, as presented in the right side of the Figure 10. These cracks propagated, and some reached total rupture, expelling material that came out of the specimens in the form of small pieces.

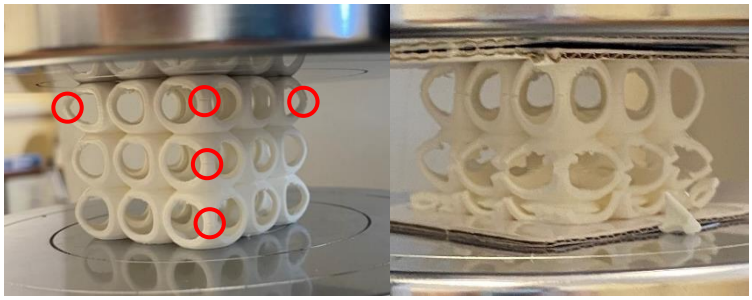

Figure 10: Example of a compression specimen during the experimental test

Concerning the failures observed in the bending specimens, two types of failure modes were registered. The first failure mode was characterized by what looks like core shear of the left side of the sandwich structure, while the second failure was also characterized probably by core shear but on the right side of the sandwich structure.

Figure 11 shows the beginning of fractures in two sections of the unit cells, which appear to be almost symmetrical concerning the midplane of the unit cell. These fractures can be seen inside the red areas. After some relatively low enforced displacement, these points in the unit cell started to crack. It was possible to observe a plane where these cracks develop in any sandwich specimen in Figure 12.The fractures also propagate along the width of the bending specimens.

In all specimens, it is possible to verify the presence of discontinuities, in the form of lines, at a certain height of the unit cells, denoting a transition between layers, mainly in the upper part of the cells. It is in these layers where the cracks start to develop in almost all the bending specimens tested, as shown in Figure 12 between the two yellow lines, which leads one to consider that these layers could be associated with the presence of defects, possibly related to overhangs.

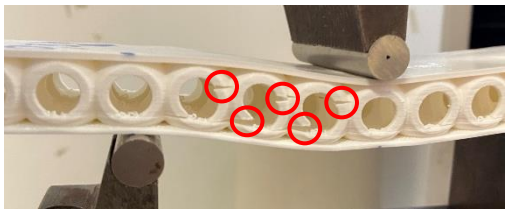

Figure 11: Start of fractures in the unit cells during a bending experimental test

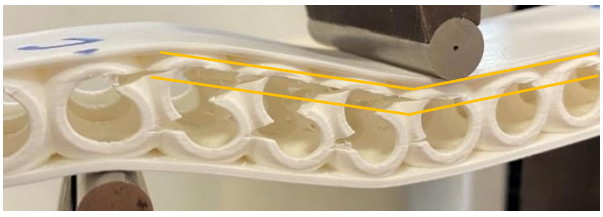

Figure 12: Failure observed in a sandwich panel, with unit cells rotated in a certain plane of failure

Comparison between numerical and experimental

Figure 13 and Figure 14 shows the comparison between the numerical and experimental results for all the specimens tested for both compression and 3-point-bending tests, respectively. Each group of specimens with the same relative density is presented in the same color but with different shades.

Observing the curves, there is a tendency, i.e., as the relative density increases, the reaction load also increases.

Table 4 shows the relative stiffness and relative energy absorbed for each specimen of both compression and bending tests and simulations, which means that the parameters were scaled by the relative density.

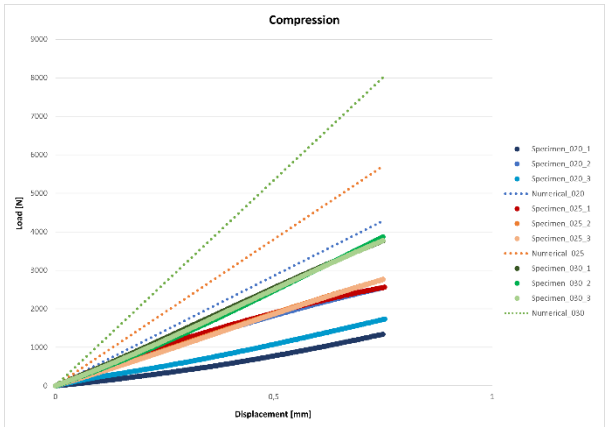

Figure 13: Comparison between the numerical and experimental load vs displacement curves of compression specimens

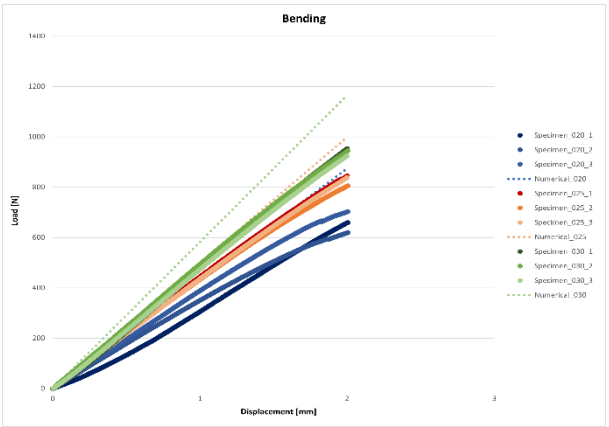

Figure 14: Comparison between the numerical and experimental load vs displacement curves of bending specimens

Table 4: Experimental and numerical relative results regarding the relative density, for both compression and bending specimens

Relative density	Compression				Bending			
	Experimental		Numerical		Experimental		Numerical	
	K / ρ_{rel}	E_{abs} / ρ_{rel}	K / ρ_{rel}	E_{abs} / ρ_{rel}	K / ρ_{rel}	E_{abs} / ρ_{rel}	K / ρ_{rel}	E_{abs} / ρ_{rel}
0.20	12492.71	3.515	28544.19	8.030	1651.49	3.302	2186.39	4.375
0.25	14382.92	4.045	30423.52	8.556	1658.99	3.320	1998.48	4.000
0.30	16896.02	4.750	35566.57	10.003	1568.01	3.137	1940.58	3.880

Overall, in the compression specimens, the mechanical properties increase with increasing the relative density and its effect on the properties is considerable. In contrast, in the bending specimens, with increasing relative density, the mechanical properties decrease but the variation is almost negligible.

The differences observed in the compression results may be associated with the design differences. The 0.30 unit cells have a shell thickness 50% thicker than the 0.20 unit cells and 15% thicker than the 0.25 unit cells. Also, the thickness of the circular crowns presented in all six faces of the 0.30 unit cells, i.e., the region of interface and connection between cells, is 25% greater compared to the 0.20 and 0.25 specimens.

This leads to the conclusion that the geometrical parameters of the unit cells design have a greater influence on the mechanical properties when subjected to compression, than when subjected to bending in the core of sandwich panels. It can also be concluded that the skins of the sandwich panels, which are the same in the three different specimens, may influence the small variation of the results, i.e., to have a greater variation of results, there must be greater variation of the relative density of the cells of the core.

Although the trend of the experimental and numerical results is similar, it is important to note that this level of differences between both are expected, mainly due to the FFF process that produces a non-isotropic material. Hence, the specimens obtained from the FFF are typically non-uniform at different levels and directions, while the finite element software considers the cells as isotropic solids. Also, the PLA material printed can have different values of mechanical properties compared to the ones chosen on Siemens NX, which may not be the most suitable.

5. Conclusions and future work

In this thesis, a TPMS unit cell was designed, based on a literature work, with three different values of relative density, in order to study the influence of the relative density of the unit cell on the mechanical properties of two different types of specimens tested. The first, a cubic specimen subjected to compression tests and the second, a sandwich panel subjected to three-point bending tests. Both experimental tests and numerical simulations were performed for both specimens, to analyse their failure behaviour and mechanical response. The unit cell was manufactured with a FFF process, through a 3D printing machine, with the appropriate parameters, chosen after an iterative selection process.

Regarding the compression specimens, both experimental and numerical results show a similar pattern between them, i.e., with increasing the relative density, the reaction load, stiffness K and energy absorbed also increase. The relative energy absorbed and relative stiffness are also directly proportional to the relative density, with the 0.30 showing the best mechanical properties, mainly in the numerical simulations. The failure observations in all compression specimens have shown that they failed at half-height of the unit cells, which is consistent with von Mises stresses presented in the same regions of the cells, from the simulations results. Also, some small pieces of material were expelled during the experimental tests and two failure modes were observed, characterized by starting to fail in the lower or upper row of cells in a horizontal plane.

Concerning the bending testtts, a tendency was observed in both experimental and numerical results. The mechanical properties showed a decrease with increasing relative density. However, there was a small variation of the results, also in the relative properties. The skins of the panels may influence this variation of the results, i.e., to have a greater variation of results, there must be greater variation of the relative density of the cells of the core. The failure behaviour observed in all bending specimens was associated with discontinuities presented at specific layers and height of the unit cells. These details are probably associated with 3D printing limitations, mainly overhangs, since it is in this upper region of the unit cells that overhangs appear.

In brief, the geometrical parameters of the unit cells design have a greater influence on the mechanical properties when subjected to compression, than when subjected to bending in the core of sandwich panels, mainly regarding the region of connection between cells.

Finally, the experimental results obtained in this work are close to those obtained by the literature work from which the unit cell of this thesis is inspired. The numerical results achieved present much higher values, in terms of applied load and stiffness, which may be related to the input and configurations made in the simulations, namely in the mechanical properties of the material used and defined in the software.

Future work should consist in further studies about the relation between the design parameters and the mechanical properties. Design optimization of the unit cell could be a good methodology to improve the performance of the unit cell. In addition, different ways of packing the unit cells would be interesting to study, as well as improve the connections between the unit cells by adding, for example, fillets in the geometry of the contact faces. It would also be interesting to study a graded lattice structure composed of the unit cells studied, by mixing relative densities in the same structure or even different geometries of cells. Also, analysing the printed specimens in an SEM microscope would be very interesting, to investigate defects and relate them to the experimental and numerical results.

6. References

[1] L. J. Gibson and M. F. Ashby, *Cellular Solids*, Second. Cambridge, UK: Cambridge University Press, 1997.

[2] M. Benedetti, A. du Plessis, R. O. Ritchie, M. Dallago, S. M. J. Razavi, and F. Berto, “Architected cellular materials: A review on their mechanical properties towards fatigue-tolerant design and fabrication,” Materials Science and Engineering R: Reports, vol. 144. Elsevier Ltd, Apr. 01, 2021, doi: 10.1016/j.mser.2021.100606.

[3] H. Yazdani Sarvestani, A. H. Akbarzadeh, H. Niknam, and K. Hermenean, “3D printed architected polymeric sandwich panels: Energy absorption and structural performance,” *Compos. Struct.*, vol. 200, no. April, pp. 886–909, 2018, doi: 10.1016/j.compstruct.2018.04.002.

[4] S. Chen, O. P. L. McGregor, A. Endruweit, L. T. Harper, and N. A. Warrior, “Simulation of the forming process for curved composite sandwich panels,” *Int. J. Mater. Form.*, vol. 13, no. 6, pp. 967–980, 2020, doi: 10.1007/s12289-019-01520-4.

[5] A. Kumar, L. Collini, A. Daurel, and J. Y. Jeng, “Design and additive manufacturing of closed cells from supportless lattice structure,” *Addit. Manuf.*, vol. 33, p. 101168, May 2020, doi: 10.1016/j.addma.2020.101168.

[6] A. Kumar, S. Verma, and J. Y. Jeng, “Supportless lattice structures for energy absorption fabricated by fused deposition modeling,” *3D Print. Addit. Manuf.*, vol. 7, no. 2, pp. 85–96, 2020, doi: 10.1089/3dp.2019.0089.

[7] “TWI - What is additive manufacturing ?” https://www.twi-global.com/technical-knowledge/faqs/what-is-additive-manufacturing#TheAdvantagesofusingAdditiveManufacturing (accessed Mar. 16, 2021).

[8] “ISO/ASTM 52900 - Additive manufacturing — General principles — Terminology.” ISO/ASTM International, 2015.

[9] “ASTM Standard: D1621 − 16 - Standard Test Method for Compressive Properties of Rigid Cellular Plastics.” ASTM International.

[10] “ASTM Standard: C 393 – 00 - Standard Test Method for Flexural Properties of Sandwich Constructions.” ASTM International.